THE JOURNAL OF PHYSICAL CHEMISTRY Letters

Letter

pubs.acs.org/JPCL

Nuclear Quantum Effects in Water at the Triple Point: Using Theory as a Link Between Experiments

Bingqing Cheng,[†] Jörg Behler,[‡] and Michele Ceriotti*[,†]

[†]Laboratory of Computational Science and Modelling, Institute of Materials, Ecole Polytechnique Fédérale de Lausanne, 1015 Lausanne, Switzerland

[‡]Lehrstuhl für Theoretische Chemie, Ruhr-Universität Bochum, 44801 Bochum, Germany

Supporting Information

ABSTRACT: One of the most prominent consequences of the quantum nature of light atomic nuclei is that their kinetic energy does not follow a Maxwell−Boltzmann distribution. Deep inelastic neutron scattering (DINS) experiments can measure this effect. Thus, the nuclear quantum kinetic energy can be probed directly in both ordered and disordered samples. However, the relation between the quantum kinetic energy and the atomic environment is a very indirect one, and cross-validation with theoretical modeling is therefore urgently needed. Here, we use state of the art path integral molecular dynamics techniques to compute the kinetic energy of hydrogen and oxygen nuclei in liquid, solid, and gas-phase water close to the triple point, comparing three different interatomic potentials and validating our results against equilibrium isotope fractionation measurements. We will then show how accurate simulations can draw a link between extremely precise fractionation experiments and DINS, therefore establishing a reliable benchmark for future measurements and providing key insights to increase further the accuracy of interatomic potentials for water.

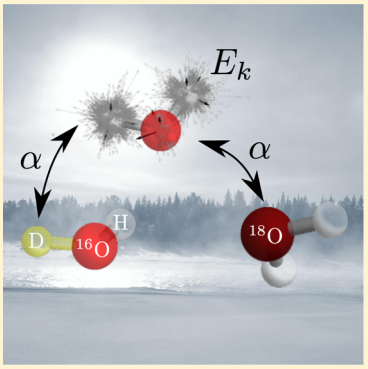

The nuclear kinetic energies (NKEs) characterize how the short-time dynamical behavior of nuclei in a physical system differs from the classical point-mass description. When the thermal energy k_BT considerably exceeds a quantum of energy $\hbar\omega$ in any vibrational mode with frequency ω, the kinetic energy distribution of nuclei follows closely the Maxwell−Boltzmann distribution. Otherwise, the mean NKE $\langle E_k \rangle$ can deviate significantly from the classical predictions, especially for light elements at or below room temperature. These nuclear quantum effects (NQEs) on kinetic energies play a crucial role in numerous phenomena such as the isotope effect,[1] hydrogen transfer rates,[2] and the heat capacity of solids.[3]

The mean NKE $\langle E_k \rangle$ can be determined from the single particle momentum distribution $n(p)$, which in turn can be measured in Deep Inelastic Neutron Scattering (DINS) experiments from the high energy and momentum transfer between neutrons and condensed matter samples.[4,5] Recently, DINS techniques have been employed to study liquid, ice, and supercritical liquid water.[6−12] Besides experimental investigations, NKEs can also be obtained from path integral molecular dynamics (PIMD) simulations, which have been used to probe NQEs in water and other hydrogen-bonded systems.[13−22] In this study, we demonstrate that $\langle E_k \rangle$ can be calculated with remarkable accuracy from PIMD simulations to establish a reference for DINS experiments. We will focus in particular on water in the vicinity of its solid−liquid transition because, in recent years, several controversial DINS studies have suggested that a large excess of NKE can be observed for protons in supercooled water,[23−26] whereas both thermodynamic arguments and simulations do not predict large anomalies in the NKE of water close to freezing.[27] Very recent experiments have carefully revisited the measurement of proton momentum distribution in water around its triple point, showing that early results were indeed overestimating significantly the NKE of supercooled water.[28] Therefore, it is highly desirable to provide a comprehensive theoretical assessment of these properties to provide much-needed cross-validation between DINS, simulations, and other less direct experimental probes of the NKE (such as inelastic neutron scattering[11,29]).

In order to accurately describe the many subtle effects contributing to the peculiar properties of water, many models have been developed over the years, ranging from single-site coarse-grained models[30] to sophisticated many-body expansions[31,32] and the on-the-fly solution of the electronic structure problem using increasingly accurate levels of theory.[33,34] In the present study, we selected three of such potentials. q-TIP4P/F is a flexible water model designed for path integral simulations[35] based on the very successful TIP4P model.[36] It uses point charges, a harmonic term for the bending, and a truncated Morse term for the OH stretch.[35] MB-pol is a polarizable potential built upon the many-body expansion of the interaction energy of water molecules, starting with the spectroscopically accurate Partridge-Schwenke (PS) monomer

Received: April 1, 2016
Accepted: May 20, 2016
Published: May 20, 2016

DOI: 10.1021/acs.jpclett.6b00729
J. Phys. Chem. Lett. 2016, 7, 2210−2215

surface,[37] and introducing two and three-body terms evaluated at the CCSD(T) level[38,39] Finally, for the present study, we have constructed a flexible and fully dissociable neural-network (NN) potential[40] following the procedure described by Morawietz et al.[41] It has been trained to represent energies and forces of the liquid and ice phases of water computed at the hybrid density functional theory level (B3LYP functional[42] with D3 dispersion corrections[43]). Further details on the ab initio reference and the NN potential, including details on the generation of the reference data set[44] and an assessment of its accuracy by out-of-sample validation can be found in the Supporting Information.

Although these models have already proven their accuracy in predicting many of the physicochemical properties of water, including its melting temperature and liquid density at room temperature,[32,35] we will first determine a quantity that is both intimately connected to the quantum kinetic energy of nuclei, and can be measured experimentally with exquisite accuracy, namely, the equilibrium isotope fractionation ratio.[45] The isotope fractionation ratio between two phases A and B $\alpha_{A-B} = \exp\left(-\frac{\Delta G_{A-B}}{k_B T}\right)$ describes the relative abundance of two isotopes X and X′ in the two environments, as given by the equilibrium

$$X_A + X'_B \rightleftharpoons^{\Delta G_{A-B}} X_B + X'_A \quad (1)$$

Using thermodynamic integration with respect to the isotope mass μ, the fractionation ratio α_{A-B} is related to $\langle E_k \rangle$ by

$$-k_B T \ln(\alpha_{A-B}) = \int_m^{m'} \frac{\langle E_k \rangle_{B,\mu}}{\mu} - \frac{\langle E_k \rangle_{A,\mu}}{\mu} d\mu \quad (2)$$

where m and m' are the masses for X and X′, respectively.

Both the isotope fractionation ratios and $\langle E_k \rangle$ can be computed from PIMD, as implemented in i-PI.[46,47] We used a NVT setup, with the water density kept at the experimental value for the various phases, a time step of 0.25 fs and constant-temperature sampling enforced by a PILE-G thermostat[47] with a time constant of 10 fs for the global centroid thermostat.[48] Sampling efficiency was further enhanced by optimal-coupling colored noise thermostats applied to each bead.[49] Simulations of liquid water and ice Ih included 256 and 360 molecules, respectively, the latter using a proton-disordered configuration from ref.[50] For the vapor, we simulated an individual molecule in vacuum, except close to the critical point, where we used nine molecules at the experimental vapor density. Many strategies can be used to reduce the computational cost of computing isotope fractionation ratios, but we restricted ourselves to conventional PIMD, given the benchmark nature of these calculations. We used 32 imaginary time slices, which have been shown to be sufficient to converge fractionation ratios around room temperature,[18] together with a recently developed scaled-coordinates estimator to evaluate α_{A-B} directly.[51] Essentially, for each of the two environments A and B one separately performs a virtual isotope substitution between one atom of type X and its isotope X′, and computes the isotope fractionation as the ratio of the corresponding partition functions. For $^{16}O/^{18}O$ fractionations, we could perform $^{16}O \rightarrow ^{18}O$ forward substitutions on all the oxygen atoms in a system containing only $H_2{}^{16}O$ molecules. As discussed in ref.,[51] in the case of H/D fractionation one has to pay particular attention to the statistical properties of the estimator, that can make the direct substitution less efficient. Rather than going directly from H to D, we performed the substitution in three stages: starting from from a system containing one atom of deuterium with all of the others being hydrogen, we performed simulations with the intermediate masses $m_1 = 1.164m_H$, $m_2 = 1.372m_H$, $m_3 = 1.641m_H$, and effectively computed the fractionation ratio as the product of the estimates for smaller mass increments $\alpha_{A-B}^{m_H \rightarrow m_D} = [\alpha_{A-B}^{m_D \rightarrow m_1} \alpha_{A-B}^{m_1 \rightarrow m_2} \alpha_{A-B}^{m_2 \rightarrow m_3} \alpha_{A-B}^{m_3 \rightarrow m_H}]^{-1}$, given that $m_D = 1.9984m_H$.

A subtle point is that, due to the symmetry of the lattice in ice Ih and to proton disorder, different sites are not fully equivalent. Computing isotope fractionation by substituting a proton in a single site could thus lead to systematic errors. In the case of $^{16}O/^{18}O$ fractionation, the possibility of performing a direct substitution resolves this problem because one can attempt substitutions at all sites from a single simulation. For the case of H/D fractionation, we used quantum alchemical exchanges to sample all sites[52] without the need of performing multiple simulations.

Figure 1 shows the fractionation ratios of H/D and $^{16}O/^{18}O$ at the triple point between vapor (V), liquid (L), and solid (S)

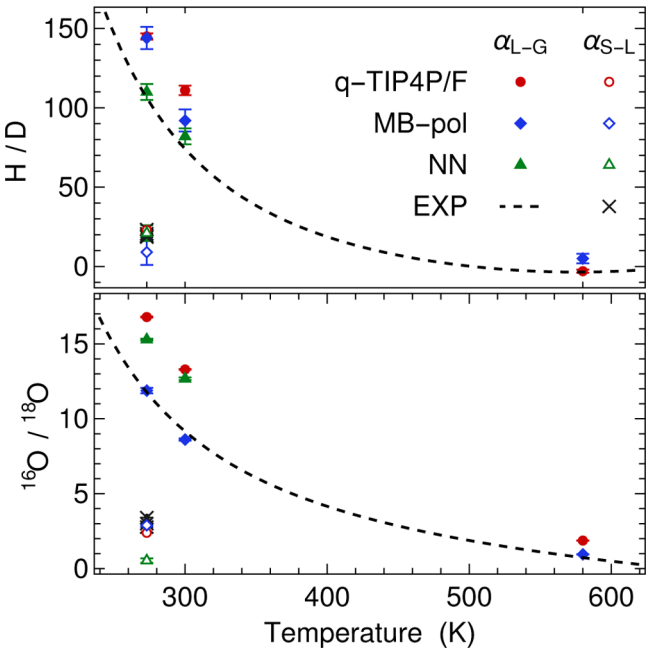

Figure 1. Isotope fractionation ratio of H/D and $^{16}O/^{18}O$ between liquid and vapor phases (filled symbols) and between ice and liquid phases (hollow symbols) of water. Note that α_{S-V}, which is not plotted here, can be simply deduced from the relation $1000\ln(\alpha_{S-V}) = 1000\ln(\alpha_{S-L}) + 1000\ln(\alpha_{L-V})$. Statistical errors are indicated in error bars. The isotope ratios on the vertical axes are expressed as $1000\ln(\alpha_{A-B})$. Three different water models were used, and experimental (EXP) values are taken from a number of studies.[53−57] All of the values, and their statistical error bars, are also presented in table form in the SI.

phases of water and the ratios between liquid and vapor at two higher temperatures (300 and 580 K) along the coexistence line. Let us first discuss the results for H/D fractionation. The NN potential, that had been trained against B3LYP+D3 ab initio calculations, matches almost perfectly the experimental results. At 300 K, it is very close to the value of 95 reported in ref 20, where first-principles forces had been used directly. Also, the raw value of $\langle E_k \rangle$ of H in liquid water at 300 K yields a value of 153.17 ± 0.08 meV, that compares very favorably to the

DOI: 10.1021/acs.jpclett.6b00729
J. Phys. Chem. Lett. 2016, 7, 2210−2215

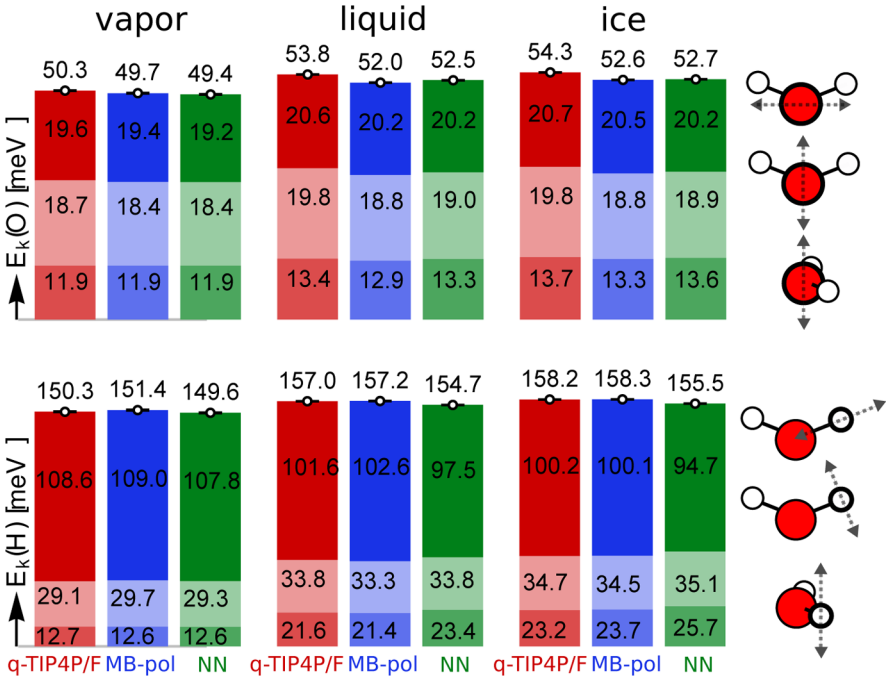

Figure 2. Average quantum kinetic energy $\langle E_k \rangle$ of the hydrogen and the oxygen atoms in three phases of water at the triple point. The error bars of total $\langle E_k \rangle$ are smaller than the symbols. The kinetic energies for each principal component of the tensor are indicated using different shades of colors, and the approximate orientations of the eigenvectors are illustrated on the right-hand side of the plot.

value of 153.3 ± 0.07 meV in ref 20. It is hard to tell whether the small difference is due to limitations of the NN training procedure, to the many approximations that had to be performed in ref 20 to cope with the large computational cost of a hybrid-functional density functional calculation, or just to statistical uncertainty. It is worth stressing that although discrepancies are noticeable on the scale of Figure 1, obtaining this level of agreement actually indicates exceptionally good performance of all the three potentials. Isotope fractionation ratios correspond to tiny free energy differences, and even an error of about ±30 in $1000\ln(\alpha_{A-B})$ translates to an error of less than 1 meV in ΔG at 273 K.

It is remarkable that q-TIP4P/F, despite being computationally inexpensive and employing a very simple parametrization of intermolecular forces, yields a rather accurate estimate for the fractionation ratios, with an overestimation of about 25% at 273 K, and correctly predicts reverse fractionation at 580 K. As discussed in ref 18, the crucial aspect is the anharmonic description of the O−H covalent bond, enabling to capture the competition between the red-shift of the stretch and the constraining of librational modes upon condensation. Simply modifying the stretching potential with a purely harmonic form leads to dramatic deterioration of the performance of q-TIP4P/F. MB-Pol overestimates the liquid−vapor H/D fractionation ratio for all temperatures from freezing to the critical point. One possible explanation for the slight overestimation of fractionation ratios by q-TIP4P/F and MB-pol is that both potentials, contrary to the NN, cannot describe bond breaking/making events and therefore fail to fully capture the softening of the covalent O−H bond in the condensed phase, that is triggered by quantum fluctuations.[58] When it comes to the fractionation of oxygen isotopes, MB-pol produces the most accurate results, in perfect agreement with experiments. Both q-TIP4P/F and the NN overestimate slightly the $^{16}O/^{18}O$ liquid−vapor fractionation. For both hydrogen and oxygen fractionation, all the models yield results that match closely the solid−liquid fractionation.

Strictly speaking, the fractionation ratio reports on a difference in (free) energy differences, and so it does not provide a stringent quantitative benchmark of the absolute NKEs in the different phases. In order to draw a link between these quantities, one should assume that one of the computed kinetic energies is exact (which is reasonable for MB-pol in the gas phase, which uses the most accurate potential energy surface available for the water molecule[37]) and that the isotope substitution can be described in a quasi-harmonic fashion (which is consistent with the dependence of $\langle E_k \rangle$ on mass, as discussed in ref 59). On the basis of these two assumptions, one finds for the liquid/vapor equilibrium

$$\langle E_k \rangle_L(H) - \langle E_k \rangle_V(H) \approx \frac{k_B T \ln \alpha_{L-V}}{2(1 - \sqrt{m_H/m_D})} \quad (3)$$

This estimate yields $\langle E_k \rangle_L(H)$ = 151.7, 153.6, and 172.3 meV at 273 K, 300 and 580 K, to be compared with 153.45 ± 0.03, 155.03 ± 0.06, and 173.68 ± 0.05 meV for MB-pol—a very good agreement despite the assumptions being made. For oxygen, the agreement is even better, with $\langle E_k \rangle_L(O)$ = 51.5, 54.6, and 87.4 meV at 273 K, 300 and 580 K estimated using eq 3, and $\langle E_k \rangle_L(O)$ = 51.50 ± 0.01, 54.55 ± 0.02, and 87.47 ± 0.01 meV for MB-pol, respectively. Using eq 3, we report in the SI a "calibration curve" that approximates the kinetic energies of O and H in liquid water from the triple point to the critical point along coexistence line based on fully converged PIMD simulations for gas phase water and experimental fractionation data. Conversely, eq 3 can also be used to approximate the fractionation ratio α_{L-V} when the cost of a rigorous estimator is prohibitive.

In the light of the extreme sensitivity of fractionation experiments on the details of the interatomic potential and the fact that in the case of water the value of α is the result of a

DOI: 10.1021/acs.jpclett.6b00729
J. Phys. Chem. Lett. 2016, 7, 2210−2215

subtle cancellation between competing quantum effects on different vibrational modes,[17,18,20,35] we would like to argue that one does not even need to invoke a direct, approximate link to the fractionation ratio through eq 3. The fact that three water models based on radically different design principles give results that are consistent with each other and with experimental data gives us great confidence in the fact that they all capture the essential physics that is necessary to describe reliably the quantum nature of nuclei in the liquid, solid, and gas phases of water.

We can then proceed to focus on the analysis of $\langle E_k \rangle$ for hydrogen and oxygen in the three phases of water at the triple point. Because we want to propose these calculations as the yardstick of future simulations and experiments, we increased the number of PIMD replicas to 64. The change relative to the kinetic energies reported above is of the order of a couple of millielectrovolts. Although the impact on fractionation ratios is much smaller (the two phases change by a very similar amount) it is important to stress that as the accuracy of DINS measurements increases,[28] it will be necessary to push PIMD beyond the level of convergence that is typically deemed sufficient for other experimental observables. For each atom, we computed the centroid virial quantum kinetic energy tensor $\mathbf{T}_{CV}$.[60,61] The mean nuclear kinetic energy can be estimated from $\langle E_k \rangle = \langle \mathrm{Tr}(\mathbf{T}_{CV}) \rangle$. Along with $\langle E_k \rangle$, the eigenvalues of $\mathbf{T}_{CV}$ can also be inferred from the nuclear momentum distribution $n(p)$ measured in DINS experiment.[19] However, the raw $\mathbf{T}_{CV}$ matrices computed in simulations can not be directly used to obtain the eigenvalues. Instantaneous values of the centroid-virial estimator are not physically meaningful, so one needs to either perform a moving average (the so-called transient anisotropic Gaussian approximation[61]) or average $\mathbf{T}$ after rotating it in the reference frame of the centroid of each water molecule, which we did here.

Figure 2 shows $\langle E_k \rangle$ for oxygen and hydrogen in the vapor, liquid, and ice phases of water at the triple point. Note that the $\langle E_k \rangle$ were obtained from averaging over all the oxygen and hydrogen atoms in the system to improve statistics and to account for the presence of slightly different environments in ice Ih. Figure 2 also illustrates the directions of the eigenvectors of $\mathbf{T}$ in the molecular frame, which correspond roughly to the main vibrational modes of each atom. It can be seen that q-TIP4P/F, MB-pol, and NN potentials all provide very similar predictions for $\langle E_k \rangle$ and the eigenvalues of $\mathbf{T}$. The consistency between the different models further confirms the reliability of our computational framework, and indicates that PIMD simulations of water can be used as a benchmark for state-of-the-art DINS experiments.

The kinetic energy decomposition in Figure 2 allows us to discuss further the small differences between the three models, and the origin of minute discrepancies in the prediction of the isotope fractionation ratios. MB-pol is very accurate in accounting for three-body terms and polarizable electrostatics, whereas q-TIP4P/F ignores them altogether, and our present NN parametrization is based on a rather basic semiempirical description of dispersion. The more accurate description of long-range, many-body effects by MB-pol is reflected in a smaller value of the softer component of the O kinetic energy tensor in the liquid, that avoids the overestimation of α_{L-V} for $^{16}O/^{18}O$ observed for the other models. On the other hand, the NN water model is the only one that allows in principle to break the covalent O−H bond. This leads to a significant decrease of the kinetic energy along the OH direction upon condensation, that is only partially compensated by the increase of the orthogonal components. The nondissociable q-TIP4P/F and MB-pol do not capture fully this softening, which justifies the overestimated α_{L-V} for H/D.

In summary, we showed that PIMD simulations can be a powerful tool for analyzing the nuclear quantum effects on NKEs. The main bottleneck of this type of simulations is that kinetic energy differences between thermodynamic states are often small, so that interatomic potentials of high accuracy are a necessary prerequisite. Equilibrium isotope fractionation provides an exquisitely sensitive benchmark of the quality of a potential in modeling quantum fluctuations and is closely related to the mean kinetic energy $\langle E_k \rangle$. The three water models we compared in the present study, namely q-TIP4P/F, MB-pol, and a neural-network potential trained on dispersion-corrected hybrid density-functional theory, give results that are remarkably consistent with each other and with precise experimental measurements, for both H/D and $^{16}O/^{18}O$, across a wide range of temperatures. The success in reproducing fractionation ratios, with models based on widely different premises, gives us confidence in our ability to predict $\langle E_k \rangle$ for water, which is further confirmed by the fact that the three models give results that are consistently within 2 meV from each other and from a simple estimate based upon the experimental fractionation ratio and virtually exact simulations for the monomer. Therefore, the values we computed for vapor, liquid, and solid water at 273 K provide a reliable, stringent reference to quantitatively assess the accuracy of existing and future DINS experiments (both for H and for the much more challenging case of O atoms). Furthermore, this study demonstrates that machine-learning potentials fitted to first-principles energies[41] can be applied with confidence to simulations including quantum nuclear fluctuations. An analysis of the decomposition of the quantum kinetic energy tensor provides a sensitive test of different potential energy surfaces for water that can help improve further the already very successful models we have considered.

■ ASSOCIATED CONTENT

Supporting Information

The Supporting Information is available free of charge on the ACS Publications website at DOI: 10.1021/acs.jpclett.6b00729.

Construction of the neural network potential, calibration curve for $\langle E_k \rangle$ in liquid water from the triple point to the critical point, and comparison between simulation and experimental isotope fractionation data. (PDF)

■ AUTHOR INFORMATION

Corresponding Author

*E-mail: michele.ceriotti@epfl.ch.

Notes

The authors declare no competing financial interest.

■ ACKNOWLEDGMENTS

M.C. and B.C. would like to acknowledge funding from the Swiss National Science Foundation (Project ID 200021-159896) and generous allocation of CPU time by CSCS under Project IDs s466 and s553, that was used to generate the database of B3LYP structures. J.B. is grateful for support by the Cluster of Excellence RESOLV (EXC 1069) funded by the DFG. Discussions with Tobias Morawietz are gratefully acknowledged.

DOI: 10.1021/acs.jpclett.6b00729
J. Phys. Chem. Lett. 2016, 7, 2210−2215

REFERENCES

(1) Bigeleisen, J.; Wolfsberg, M. Theoretical and experimental aspects of isotope effects in chemical kinetics. *Advances in Chemical Physics* **1957**, *1*, 15−76.

(2) Liu, Y. P.; Lu, D. H.; Gonzalez-Lafont, A.; Truhlar, D. G.; Garrett, B. C. Direct dynamics calculation of the kinetic isotope effect for an organic hydrogen-transfer reaction, including corner-cutting tunneling in 21 dimensions. *J. Am. Chem. Soc.* **1993**, *115*, 7806−7817.

(3) Kremer, R.; Cardona, M.; Schmitt, E.; Blumm, J.; Estreicher, S.; Sanati, M.; Bockowski, M.; Grzegory, I.; Suski, T.; Jezowski, A. Heat capacity of α- Ga N: Isotope effects. *Phys. Rev. B: Condens. Matter Mater. Phys.* **2005**, *72*, 075209.

(4) Silver, R. N. Theory of deep inelastic neutron scattering. II. Application to normal and superfluid He 4. *Phys. Rev. B: Condens. Matter Mater. Phys.* **1989**, *39*, 4022.

(5) Andreani, C.; Colognesi, D.; Mayers, J.; Reiter, G.; Senesi, R. Measurement of momentum distribution of lightatoms and molecules in condensed matter systems using inelastic neutron scattering. *Adv. Phys.* **2005**, *54*, 377−469.

(6) Pantalei, C.; Pietropaolo, A.; Senesi, R.; Imberti, S.; Andreani, C.; Mayers, J.; Burnham, C.; Reiter, G. Proton momentum distribution of liquid water from room temperature to the supercritical phase. *Phys. Rev. Lett.* **2008**, *100*, 177801.

(7) Pietropaolo, A.; Senesi, R.; Andreani, C.; Botti, A.; Ricci, M.; Bruni, F. Excess of proton mean kinetic energy in supercooled water. *Phys. Rev. Lett.* **2008**, *100*, 127802.

(8) Andreani, C.; Colognesi, D.; Pietropaolo, A.; Senesi, R. Ground state proton dynamics in stable phases of water. *Chem. Phys. Lett.* **2011**, *518*, 1−6.

(9) Flammini, D.; Pietropaolo, A.; Senesi, R.; Andreani, C.; McBride, F.; Hodgson, A.; Adams, M. a.; Lin, L.; Car, R. Spherical momentum distribution of the protons in hexagonal ice from modeling of inelastic neutron scattering data. *J. Chem. Phys.* **2012**, *136*, 024504.

(10) Senesi, R.; Romanelli, G.; Adams, M. A.; Andreani, C. Temperature dependence of the zero point kinetic energy in ice and water above room temperature. *Chem. Phys.* **2013**, *427*, 111−116.

(11) Andreani, C.; Romanelli, G.; Senesi, R. A combined INS and DINS study of proton quantum dynamics of ice and water across the triple point and in the supercritical phase. *Chem. Phys.* **2013**, *427*, 106−110.

(12) Romanelli, G.; Fernandez-Alonso, F.; Andreani, C. The Harmonic Picture of Nuclear Mean Kinetic Energies in Heavy Water. *Journal of Physics: Conference Series* **2014**, *571*, 012003.

(13) Fanourgakis, G.; Schenter, G.; Xantheas, S. A quantitative account of quantum effects in liquid water. *J. Chem. Phys.* **2006**, *125*, 141102.

(14) Paesani, F.; Iuchi, S.; Voth, G. A. Quantum effects in liquid water from an ab initio-based polarizable force field. *J. Chem. Phys.* **2007**, *127*, 074506.

(15) Morrone, J. A.; Srinivasan, V.; Sebastiani, D.; Car, R. Proton momentum distribution in water: an open path integral molecular dynamics study. *J. Chem. Phys.* **2007**, *126*, 234504.

(16) Lin, L.; Morrone, J. A.; Car, R. Correlated Tunneling in Hydrogen Bonds. *J. Stat. Phys.* **2011**, *145*, 365−384.

(17) Li, X.-Z.; Walker, B.; Michaelides, A. Quantum nature of the hydrogen bond. *Proc. Natl. Acad. Sci. U. S. A.* **2011**, *108*, 6369−6373.

(18) Markland, T. E.; Berne, B. Unraveling quantum mechanical effects in water using isotopic fractionation. *Proc. Natl. Acad. Sci. U. S. A.* **2012**, *109*, 7988−7991.

(19) Romanelli, G.; Ceriotti, M.; Manolopoulos, D. E.; Pantalei, C.; Senesi, R.; Andreani, C. Direct Measurement of Competing Quantum Effects on the Kinetic Energy of Heavy Water upon Melting. *J. Phys. Chem. Lett.* **2013**, *4*, 3251−3256.

(20) Wang, L.; Ceriotti, M.; Markland, T. E. Quantum fluctuations and isotope effects in ab initio descriptions of water. *J. Chem. Phys.* **2014**, *141*, 104502.

(21) Pinilla, C.; Blanchard, M.; Balan, E.; Ferlat, G.; Vuilleumier, R.; Mauri, F. Equilibrium fractionation of H and O isotopes in water from path integral molecular dynamics. *Geochim. Cosmochim. Acta* **2014**, *135*, 203−216.

(22) Rossi, M.; Fang, W.; Michaelides, A. Stability of Complex Biomolecular Structures: van der Waals, Hydrogen Bond Cooperativity, and Nuclear Quantum Effects. *J. Phys. Chem. Lett.* **2015**, *6*, 4233−4238.

(23) Pietropaolo, A.; Senesi, R.; Andreani, C.; Botti, A.; Ricci, M. a.; Bruni, F. Excess of Proton Mean Kinetic Energy in Supercooled Water. *Phys. Rev. Lett.* **2008**, *100*, 2−5.

(24) Pietropaolo, A.; Senesi, R.; Andreani, C.; Botti, A.; Ricci, M. A.; Bruni, F.; et al. Reply to the Comment by A. K. Soper. *Phys. Rev. Lett.* **2009**, *103*, 69802.

(25) Soper, A. K. Comment on "Excess of Proton Mean Kinetic Energy in Supercooled Water". *Phys. Rev. Lett.* **2009**, *103*, 69801.

(26) Flammini, D.; Ricci, M. a.; Bruni, F. A new water anomaly: the temperature dependence of the proton mean kinetic energy. *J. Chem. Phys.* **2009**, *130*, 236101.

(27) Ramírez, R.; Herrero, C. P. Kinetic energy of protons in ice Ih and water: A path integral study. *Phys. Rev. B: Condens. Matter Mater. Phys.* **2011**, *84*, 064130.

(28) Andreani, C.; Romanelli, G.; Senesi, R. Direct measurements of quantum kinetic energy tensor in stable and metastable water near the triple point: an experimental benchmark. *J. Phys. Chem. Lett.* **2016**, DOI: 10.1021/acs.jpclett.6b00926.

(29) Senesi, R.; Flammini, D.; Kolesnikov, A. I.; Murray, É D.; Galli, G.; Andreani, C. The quantum nature of the OH stretching mode in ice and water probed by neutron scattering experiments. *J. Chem. Phys.* **2013**, *139*, 074504.

(30) Molinero, V.; Moore, E. B. Water Modeled As an Intermediate Element between Carbon and Silicon. *J. Phys. Chem. B* **2009**, *113*, 4008−4016.

(31) Wang, Y.; Bowman, J. M. Towards an ab initio flexible potential for water, and post-harmonic quantum vibrational analysis of water clusters. *Chem. Phys. Lett.* **2010**, *491*, 1−10.

(32) Medders, G. R.; Babin, V.; Paesani, F. Development of a "First-Principles" Water Potential with Flexible Monomers. III. Liquid Phase Properties. *J. Chem. Theory Comput.* **2014**, *10*, 2906−2910.

(33) Del Ben, M.; Schönherr, M.; Hutter, J.; Vandevondele, J. Bulk liquid water at ambient temperature and pressure from mp2 theory. *J. Phys. Chem. Lett.* **2013**, *4*, 3753−3759.

(34) Zen, A.; Luo, Y.; Mazzola, G.; Guidoni, L.; Sorella, S. Ab initio molecular dynamics simulation of liquid water by quantum Monte Carlo. *J. Chem. Phys.* **2015**, *142*, 144111.

(35) Habershon, S.; Markland, T. E.; Manolopoulos, D. E. Competing quantum effects in the dynamics of a flexible water model. *J. Chem. Phys.* **2009**, *131*, 024501.

(36) Abascal, J. L. F.; Vega, C. A general purpose model for the condensed phases of water: TIP4P/2005. *J. Chem. Phys.* **2005**, *123*, 234505.

(37) Partridge, H.; Schwenke, D. W. The determination of an accurate isotope dependent potential energy surface for water from extensive ab initio calculations and experimental data. *J. Chem. Phys.* **1997**, *106*, 4618.

(38) Babin, V.; Leforestier, C.; Paesani, F. Development of a "First Principles" Water Potential with Flexible Monomers: Dimer Potential Energy Surface, VRT Spectrum, and Second Virial Coefficient. *J. Chem. Theory Comput.* **2013**, *9*, 5395−5403.

(39) Babin, V.; Medders, G. R.; Paesani, F. Development of a "First Principles" Water Potential with Flexible Monomers. II: Trimer Potential Energy Surface, Third Virial Coefficient, and Small Clusters. *J. Chem. Theory Comput.* **2014**, *10*, 1599−1607.

(40) Behler, J.; Parrinello, M. Generalized Neural-Network Representation of High-Dimensional Potential-Energy Surfaces. *Phys. Rev. Lett.* **2007**, *98*, 146401.

(41) Morawietz, T.; Singraber, A.; Dellago, C.; Behler, J. How van der Waals interactions determine the unique properties of water. Submitted for publication, **2016**.

(42) Becke, A. D. Density-functional thermochemistry. III. The role of exact exchange. *J. Chem. Phys.* **1993**, *98*, 5648.

DOI: 10.1021/acs.jpclett.6b00729
J. Phys. Chem. Lett. 2016, 7, 2210−2215

(43) Grimme, S.; Antony, J.; Ehrlich, S.; Krieg, H. A consistent and accurate ab initio parametrization of density functional dispersion correction (DFT-D) for the 94 elements H-Pu. *J. Chem. Phys.* **2010**, *132*, 154104.
(44) Gasparotto, P.; Hassanali, A. A.; Ceriotti, M. Probing Defects and Correlations in the Hydrogen-Bond Network of ab Initio Water. *J. Chem. Theory Comput.* **2016**, *12*, 1953−1964.
(45) Werner, R. A.; Brand, W. A. Referencing strategies and techniques in stable isotope ratio analysis. *Rapid Commun. Mass Spectrom.* **2001**, *15*, 501−519.
(46) Ceriotti, M.; More, J.; Manolopoulos, D. E. i-PI: A Python interface for ab initio path integral molecular dynamics simulations. *Comput. Phys. Commun.* **2014**, *185*, 1019−1026.
(47) Ceriotti, M.; Parrinello, M.; Markland, T. E.; Manolopoulos, D. E. Efficient stochastic thermostatting of path integral molecular dynamics. *J. Chem. Phys.* **2010**, *133*, 124104.
(48) Bussi, G.; Donadio, D.; Parrinello, M. Canonical sampling through velocity rescaling. *J. Chem. Phys.* **2007**, *126*, 014101.
(49) Ceriotti, M.; Bussi, G.; Parrinello, M. Colored-Noise Thermostats à la Carte. *J. Chem. Theory Comput.* **2010**, *6*, 1170−1180.
(50) Hayward, J. A.; Reimers, J. R. Unit cells for the simulation of hexagonal ice. *J. Chem. Phys.* **1997**, *106*, 1518−1529.
(51) Cheng, B.; Ceriotti, M. Direct path integral estimators for isotope fractionation ratios. *J. Chem. Phys.* **2014**, *141*, 244112.
(52) Liu, J.; Andino, R. S.; Miller, C. M.; Chen, X.; Wilkins, D. M.; Ceriotti, M.; Manolopoulos, D. E. A Surface-Specific Isotope Effect in Mixtures of Light and Heavy Water. *J. Phys. Chem. C* **2013**, *117*, 2944−2951.
(53) Horita, J.; Wesolowski, D. J. Liquid-vapor fractionation of oxygen and hydrogen isotopes of water from the freezing to the critical temperature. *Geochim. Cosmochim. Acta* **1994**, *58*, 3425−3437.
(54) Merlivat, L.; Nief, G. Fractionnement isotopique lors des changements d état solide-vapeur et liquide-vapeur de l'eau à des températures inférieures à 0° C. *Tellus* **1967**, *19*, 122.
(55) Majoube, M. Fractionation factor of 18O between water vapour and ice. *Nature* **1970**, *226*, 1242−1242.
(56) O'Neil, J. R. Hydrogen and oxygen isotope fractionation between ice and water. *J. Phys. Chem.* **1968**, *72*, 3683−3684.
(57) Ellehoj, M.; Steen-Larsen, H. C.; Johnsen, S. J.; Madsen, M. B. Ice-vapor equilibrium fractionation factor of hydrogen and oxygen isotopes: Experimental investigations and implications for stable water isotope studies. *Rapid Commun. Mass Spectrom.* **2013**, *27*, 2149−2158.
(58) Ceriotti, M.; Cuny, J.; Parrinello, M.; Manolopoulos, D. E. Nuclear quantum effects and hydrogen bond fluctuations in water. *Proc. Natl. Acad. Sci. U. S. A.* **2013**, *110*, 15591−6.
(59) Ceriotti, M.; Markland, T. E. Efficient methods and practical guidelines for simulating isotope effects. *J. Chem. Phys.* **2013**, *138*, 014112.
(60) Cao, J.; Berne, B. J. On energy estimators in path integral Monte Carlo simulations: Dependence of accuracy on algorithm. *J. Chem. Phys.* **1989**, *91*, 6359.
(61) Ceriotti, M.; Manolopoulos, D. E. Efficient First-Principles Calculation of the Quantum Kinetic Energy and Momentum Distribution of Nuclei. *Phys. Rev. Lett.* **2012**, *109*, 100604.

DOI: 10.1021/acs.jpclett.6b00729
J. Phys. Chem. Lett. 2016, 7, 2210−2215